PERMANENT QUADRUPOLE MAGNET FOR DRIFT TUBE LINACS

A. Noda, M. Mutou, M. Yoshizawa and A. Mizobuchi
Institute for Nuclear Study, University of Tokyo
Midoricho 3-2-1, Tanashi-city, Tokyo 188, Japan

Summary

A quadrupole magnet with use of permanent magnets is fabricated. Considering the fact that ions with different charge to mass ratio should be accepted for the case of heavy-ion linac, additional coils of 14000 AT per pole are attached to the magnet. These coils are only excited for varing the field gradient with a short pulse duration of ∿200 ms and no cooling is needed. From the point of view of controlling the field gradient, too stiff material such as $SmCo_5$ requires much larger magneto-motive force and is not suitable for the present case and AlNiCo alloy is adopted. Soft iron pole tip with circular shape is attached to permanent magnet to improve the field property.

Achieved maximum field gradient is measured at 2.1 kG/cm for a bore radius of 15 mm. The outer diameter of the whole magnet and its core length are 155 mm and 70 mm, respectively. From the result of field measurement, the higher multipole components are suppressed at tolerable size.

Introduction

For drift tube linacs, fabrication of a compact focusing quadrupole magnet is of importance so as to improve the shunt impedance by reduction of capacitance between adjacent drift tubes. From this point of view and the merit of convenience of operation without power supply and additional power dissipation due to excitation current in the coil, permanent quadrupole magnets has becoming to be developed at various laboratories as focusing elements for drift tube linacs and for the other use[1∿10].

For the case of heavy ion linacs, however, charge to mass ratio of the accelerated beam changes largely. For example, at the injector linac of NUMATRON, charge to mass ratio changes from 0.2 to 1.0 even for the Alvarez linac after 2nd stripper[11]. So focusing strength has some necessity to be variable according to ion species to be accelerated. So as to respond to this necessity of flexibility of field gradient, a permanent quadrupole magnet with additional coils is fabricated. These coils are used not for DC excitation as electric quadrupole magnet but for pulsed excitation only for the purpose of magnetization of the permanent magnet. Thus the current density in the coil can be increased and the total volume of the magnet can be made compact by reduction of coil spaces without sacrificing the flexibility of the field gradient. In fig. 1, an overall view of the fabricated magnet is given.

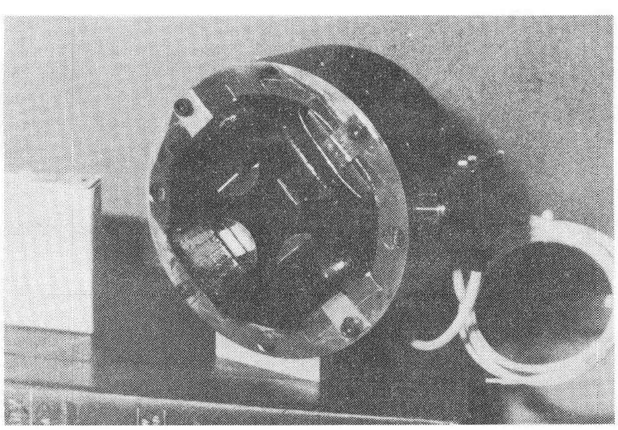

Fig. 1. Overall view of the quadrupole magnet.

In the present paper, the design of the fabricated permanent quadrupole magnet is described and then the result of field measurement with use of a rotating coil is given.

Design of the Magnet

Material of the Permanent Magnet

As the material of permanent magnet, Rare Earth-Cobalt(REC) such as $SmCo_5$ is preferable from the point of view of realizing as high field gradient as possible. However the REC is, in general, magnetically so hard that it needs large ampere-turns to change the magnetization, which is disadvantageous for the present case. So AlNiCo alloy is adopted as the material of permanent magnet, because it attains moderate field strength and its magnetization can be changed with moderate ampere-turns.

Operating Point of Permanent Magnet

The magneto-motive force of the quadrupole magnet is to be originated by blocks of permanent magnet installed in the shaded region in fig. 2. So as to reduce the effect of the alignment of magnetic domain in the permanent magnet to the field structure, a pole tip with circular shape made of soft iron is attached to each block of permanent magnet as shown in fig. 2.

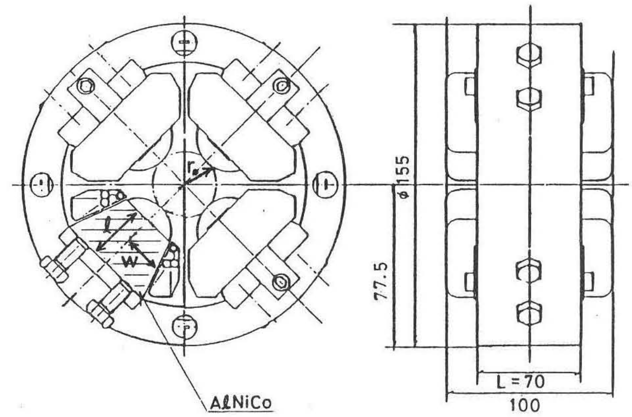

Fig. 2. Geometry of the permanent quadrupole magnet.

For the magnet with the geometry shown in fig. 2, the following relations hold;

$$H_d \cdot \ell + \frac{1}{2\mu_0} G r_0^2 = 0 \qquad (1)$$

$$B_d \cdot w \cdot L = \frac{1}{2} G x_c^2 L , \qquad (2)$$

where notations are as follows

μ_0 : permeability in the air,
G : field gradient of the quadrupole magnet,
L : core length along the magnet axis
and
x_c : the effective boundary of the magnetic field in the median plane defined by the relation: $\frac{1}{2} G x_c^2 = \int B_z(x)dx$ (fig. 3).

Combination of eqs. (1) and (2) gives

$$\frac{B_d}{H_d} = -\frac{\mu_0 \ell x_c^2}{w r_0^2} . \qquad (3)$$

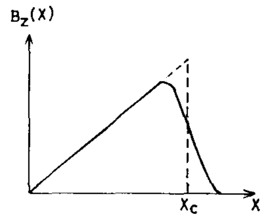

Fig. 3. Definition of the effective field boundary (x_C).

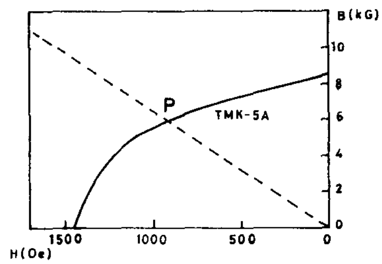

Fig. 4. Operating point and demagnetizing curve.

For the present magnet, bore radius, r_0, length and effective half width of the permanent magnet block, ℓ and w are 15 mm, 28 mm and 19.5 mm, respectively. The effective boundary of the median-plane field defined above is estimated at 32.3 mm from the result of numerical calculation with TRIM assuming the electrical magnet with the same geometry made of soft iron. This value of x_C gives 4.62 as the leakage coefficient defined by Kapchinskij et al.[1], which is in good agreement with their value of 5 . Substituting these values into eq. (3), the ratio B_d/H_d is calculated at - 6.64. Drawing a straight line with this slope on the demagnetizing curve of the AlNiCo alloy(TMK5A), the operating point, P, is obtained as shown in fig. 4. From this operating point, the field gradient realized for the quadrupole magnet is calculated at 2.2 kG/cm for full magnetizing level. This field gradient is not so high but which still covers rather wide region of Alvarez linac of NUMATRON injector with doublet focusing(FFDD).

Ampere-turns Necessary to Magnetize

The relation between the magneto-motive force induced in the permanent magnet, $H\cdot\ell$, and externally applied ampere-turns by each coil, NI, is given as

$$NI = \frac{1}{2\mu_0} G r_0^2 + H\cdot\ell \ , \qquad (4)$$

neglecting the magnetic resistance in the soft iron, in which relative permeability is so high. Combining the relation

$$\frac{1}{2} G x_C^2 L = \mu_m H w L \qquad (5)$$

with eq. (4), the required ampere-turns is expressed as

$$NI = \left(\frac{\mu_m}{\mu_0}\cdot\frac{w r_0^2}{x_C^2} + \ell\right)H \ , \qquad (6)$$

where μ_m is the permeability in the permanent magnet.

The present AlNiCo alloy is almost saturated at 3 kOe and to attain this value, required ampere-turn is calculated at 1.27×10^4 AT from eq. (6) using the dimensions of the magnet given above. As a coil with 14 turns is wound around each pole, the required current is ∿900 A and the coil is designed to allow maximum excitation of 1000 A with pulsed excitation. As the cross section of the coil conductor is chosen at rather small value of 8.04 mm^2 to reduce the coil spaces, the current density amounts to 124.4 A/mm^2 at the pulse excitation peak. From the test of pulse magnetization with a test sample of the permanent magnet, pulse duration longer than 200 msec is found to be enough for magnetization (fig. 5) and considering the fact that

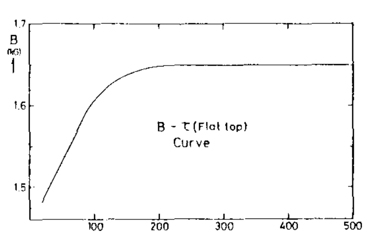

Fig. 5. Relation between duration of pulsed excitation and residual strength of the magnetic field obtained by a test sample.

this pulsed excitation is not repeated continuously but is made only one cycle for the desired magnetization level, this value is safely operated.

Field Measurement

Principle of Measurement

In the measuring system illustrated in fig. 6 where the origin of the coordinates is chosen to be the axis of the rotation and is displaced as large as Δx and Δz in x and z directions, respectively from the magnet axis, the azimuthal component of the magnetic field, B_θ, is written as[12]

$$B_\theta = -\sum_{n=1}^{\infty} n a_n r^{n-1}[\cos n\theta + \frac{n-1}{r}\{\Delta x \cos(n-1)\theta - \Delta z \sin(n-1)\theta\}] \ , \qquad (7)$$

where a_n is the expansion coefficient of magnetic scalar potential with respect to r, which is related to multipole field component as

$$\frac{d^{(n-1)}B_z}{dx^{(n-1)}} = -a_n \cdot n! \ . \qquad (8)$$

The induced voltage at the coil, ε, can be written as

$$\varepsilon = NS\omega \sum_{n=1}^{\infty} n a_n r^{n-1}[n \sin n\theta + \frac{(n-1)^2}{r}\{\Delta x \sin(n-1)\theta + \Delta z \cos(n-1)\theta\}] \ , \qquad (9)$$

where ω is the angular velocity of the rotating coil. This voltage signal is fed to Fast Fourier Transformer (FFT) through the slip ring and is frequency analysed. The rms amplitude of the n-th harmonic component is given by

$$F_n + \Delta F_n = \frac{NS\omega}{\sqrt{2}}[n^2 a_n r^{n-1} + n^2(n+1)a_{n+1}r^{n-1}\Delta r] \ . \qquad (10)$$

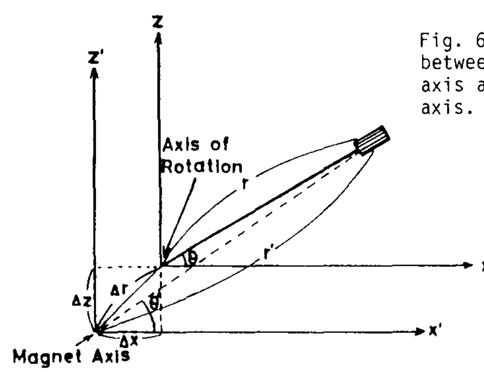

Fig. 6. Relation between rotation axis and magnet axis.

Procedure of Field Measurement

A block diagram of field measurement is given in fig. 7. The position of the rotating axis can be controlled in three dimensional space with the precision of 10 μm. Measurement is executed fixing the position in y direction at the center of the magnet core along the magnet axis with the coil with dimensions of 5 x 10 x 5.5 mm^3.

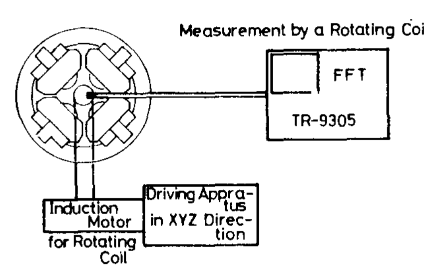

Fig. 7. Block diagram of the field measurement system with use of a rotating coil.

The position dependence of the dipole component, D(= F_1 + ΔF_1) is measured for the various position of Δx and Δz as shown in fig. 8. From the data shown by black circles, it is known that the dipole component is originated from ΔF_1, because it vanishes at the position where Δx and Δz are 0.15 mm and 0.14 mm, respectively. So the displacement of the field center from the geometrical center is estimated at ∿0.2 mm.

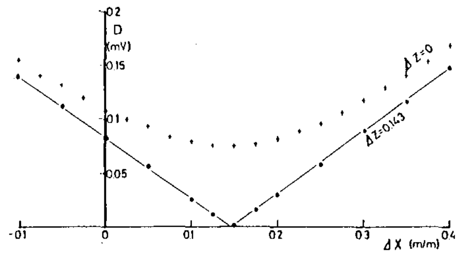

Fig. 8. Position dependence of dipole component.

The multipole components are measured fixing the rotation axis at the field center. The absolute value of the field level is scaled with use of a temperature controlled Hall-probe calibrated in a uniform field by an NMR. Typical result is illustrated in fig. 9 and is

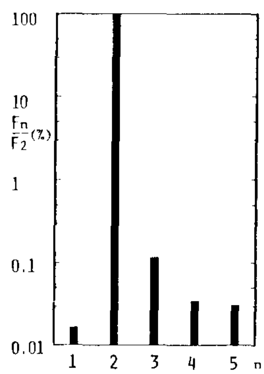

Fig. 9. Strength of multipole field signal relative to the quadrupole signal. Measurement is done by a rotating coil system. F_n in the figure represents 2n-pole field component.

listed up in table I. The field gradient realized for the present quadrupole magnet is measured at 2.1 kG/cm for full magnetization, which is in good agreement with the calculated value described before. The multipole fields other than the quadrupole component are well suppressed as is seen from table I.

TABLE I

MULTIPOLE COMPONENTS OF THE QUADRUPOLE MAGNET

Harmonic Component	Signal Level	Percentage Relative to the Quadrupole Signal	Multipole Field
Dipole	1.25 μV	0.016 %	3.8×10^{-4} kG
Quadrupole	7.60 mV	100 %	2.1 kG/cm
Sextupole	8.80 μV	0.12 %	5.9×10^{-3} kG/cm^2
Octapole	2.65 μV	0.035 %	7.3×10^{-3} kG/cm^3
Decapole	2.35 μV	0.031 %	3.8×10^{-2} kG/cm^4

Flexibility of the Field Gradient

Additional coils for pulsed excitation are wound for the present magnet to make its field gradient variable. From the test of reproducibility, it is found that a cycle of bipolar pulsed excitation which almost saturates the magnetization in the permanent magnet (major loop) is needed prior to the magnetization with appropriate excitation current so as to reproduce the same field gradient with the same excitation current independent on the previous state of magnetization. With the excitation pattern shown in fig. 10, the field gradient can be varied according to the final excitation current, X, as shown in the figure.

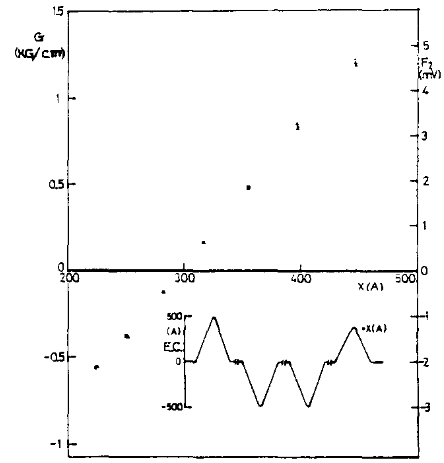

Fig. 10. Typical excitation pattern and the relation between excitation current (X) and residual quadrupole field strength (G).

Multipole fields are also measured for these field level with the rotating coil. Although undesirable field components such as dipole, sextupole, octapole etc. become a little larger (several percent) and might cause some beam dynamical problem if the field gradient goes down less than 10 % of the maximum value, it is found that these field components are well suppressed (less than 1 %) at the higher magnetization level.

Acknowlegement

The authors would like to present their sincere thanks to Prof. Y. Hirao for his suggestion about the idea of variable strength permanent magnet and continuous encouragement. They are also indebted to Mr. T. Fujino and other members of the Machine Shop at INS who have designed and fabricated the rotating coil system.

References

1. I. M. Kapchinskij, A. M. Kozodaev, N. V. Lazarev and V. S. Skachkov, "DESIGN AND DEVELOPMENT OF PERMANENT MAGNET QUADRUPOLES FOR ION LINACS," Proc. of the 1976 Linear Accel. Conf. (1976) 350.
2. E. D. Bush, Jr. "PERMANENT QUADRUPOLE MAGNETS," ibid. 363.
3. N. Saito, E. D. Bush and D. A. Swenson, "Development of Samarium-Cobalt Quadrupole Lenses for Particle Accelerator Applications," Proc. of the 3rd Intern. Workshop on Rare Earth-Cobalt Permanent Magnets and their Applications (1978).
4. K. Halbach, "STRONG RARE EARTH COBALT QUADRUPOLES," IEEE Trans. on Nucl. Sci. NS-26 No. 3 (1979) 3882.
5. R. F. Holsinger, "THE DRIFT TUBE AND BEAM LINE QUADRUPOLE PERMANENT MAGNETS FOR THE NEN PROTON LINAC," Proc. of the 1979 Linear Accel. Conf. (1979) 373.
6. N. V. Lazarev and V. S. Skachkov, "TIPLESS PERMANENT MAGNET QUADRUPOLE LENSES," ibid. 380.
7. A. N. Gerbert and S. B. Mukho, Ya. D. Rabinovich and V. S. Skachkov, "QUADRUPOLE LENS WITH POLES OF IMPLICIT FORM BASED ON PERMANENT MAGNETS," Priv. i Tekh. Eksp. No. 1 (1980) 49.
8. K. Halbach, "DESIGN OF PERMANENT MULTIPOLE MAGNETS WITH ORIENTED RARE EARTH COBALT MATERIAL," Nucl. Instr. and Meth. 169 (1980) 1.
9. R. L. Gluckstern and R. F. Holsinger, "DESIGN OF REC PERMANENT MAGNET QUADRUPOLES TAKING INTO ACCOUNT B, H NON-LINEARITY," Proc. of the 1981 Linear Accel. Conf. (1981) 214.
10. K. Halbach, " CONCEPTUAL DESIGN OF A PERMANENT QUADRUPOLE MAGNET WITH ADJUSTABLE STRENGTH," Nucl. Instr. and Meth. 206 (1983) 353.
11. Y. Hirao et al., "NUMATRON High-Energy Heavy-Ion Facility," INS-NUMA-5, PART II (1977).
12. A. Noda, M. Yoshizawa, M. Mutou and T. Fujino, "Measuring System of Multipole Fields of the Quadrupole Magnet in Drift-tubes of a Linear Accelerator," INS-NUMA-32 (1982).